Electronic Supplementary Material (ESI) for Analyst.

Supplemental Information

New Insights into the Electrochemical Detection Application of p-p Junction Foam: the Effects of Interfacial Potential Barrier

Longjiang Ding,[a] Minggang Zhao,*[a] Sisi Fan,[a] Hui Li,[b] Ye Ma,[c] Jingjing Liang[a] and Shougang Chen*[a]

[a]Department of Materials Science and Engineering, Ocean University of China, Qingdao 266100, P R China.

[b]Optoelectronic Materials and Technologies Engineering Laboratory of Shandong, Physics Department, Qingdao University of Science and Technology, Qingdao 266100, PR China

[c]Department of Chemistry, Imperial College London, London, SW7 2AZ, UK

** E-mail: Zhaomg@ouc.edu.cn*

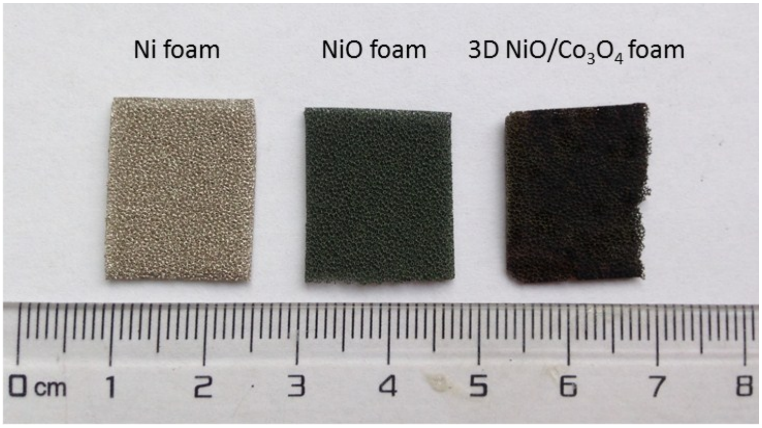

Fig. S1 Digital images of the Ni, NiO and 3D NiO/Co_3O_4 foam, obvious color change is observed during the fabricating process.

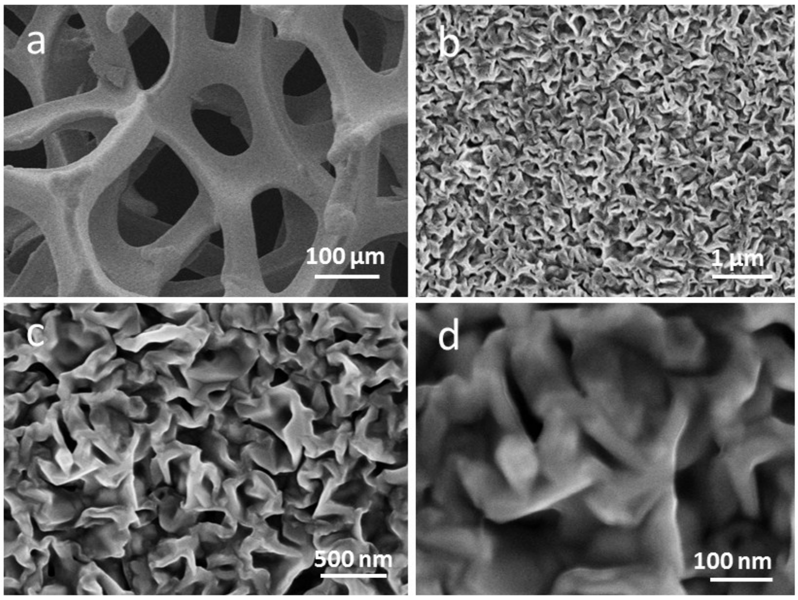

Fig. S2 Low to high magnification SEM images of NiO foam (from a to d). The bare NiO is a macro-porous skeleton with amounts of nano-wrinkles and nanopores distributed on the surface.

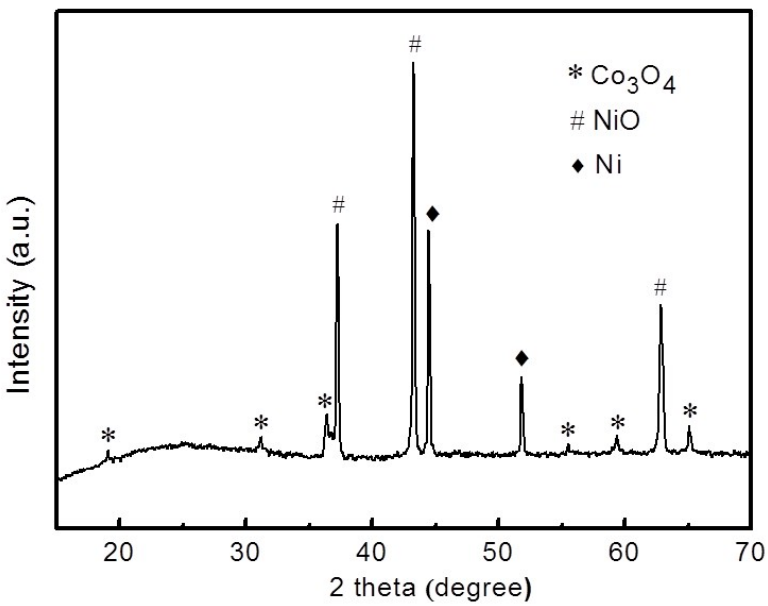

Fig. S3 The XRD spectra of 3D NiO/Co_3O_4 foam, all XRD patterns can be indexed as NiO foam and Co_3O_4, and no impurity phase appears.

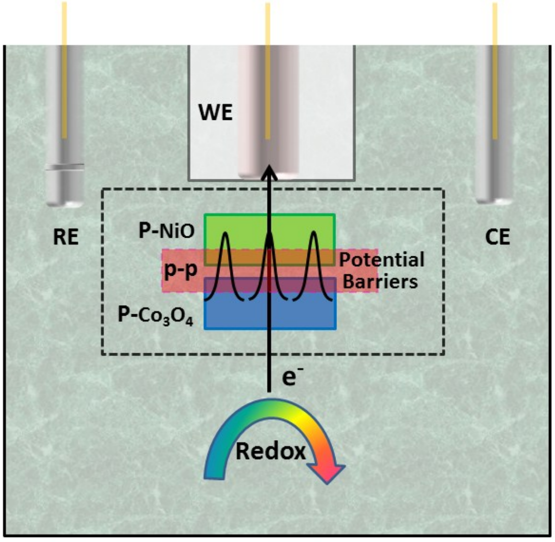

Fig. S4 The working principle of the p-p junction with functional interfacial potential barriers for the redox-based electrochemical detection.

When no redox occurred, the electrons transport pathway through the potential barrier was not built, so the adjustive effects of the potential barrier could not be triggered. When the redox occurs, the adsorbate-induced change of the potential barrier could change the resistance of the biosensors, detecting the charged molecules with high sensitivity and selectivity. Specifically, the positively charged molecules that are absorbed around the p-p junction barrier area do decrease the barrier height Φ, which results in the observed current increase. In contrast, when negatively charged molecules are introduced, a current decrease is observed.

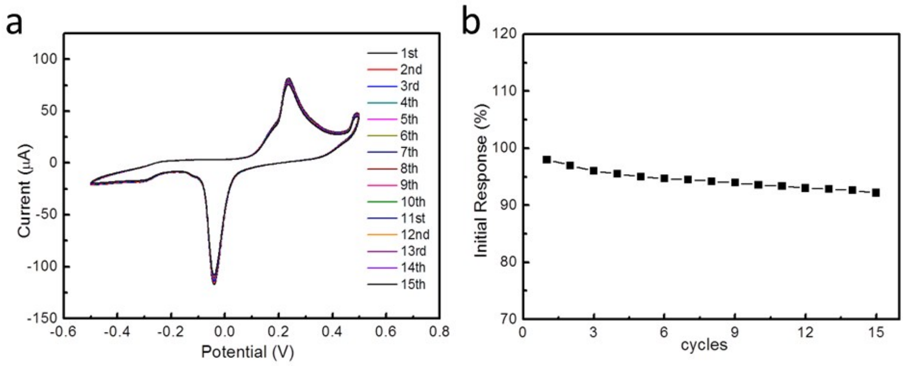

Fig. S5 CV curves (a) of the prepared biosensor based on 3D NiO/Co_3O_4 foam for 15 cycles in presence of 5 mM DA in PBS at pH 7.4. (b) The change of the response to DA by successively cycling the electrode for 15 repeated cycles, no obvious change was found.

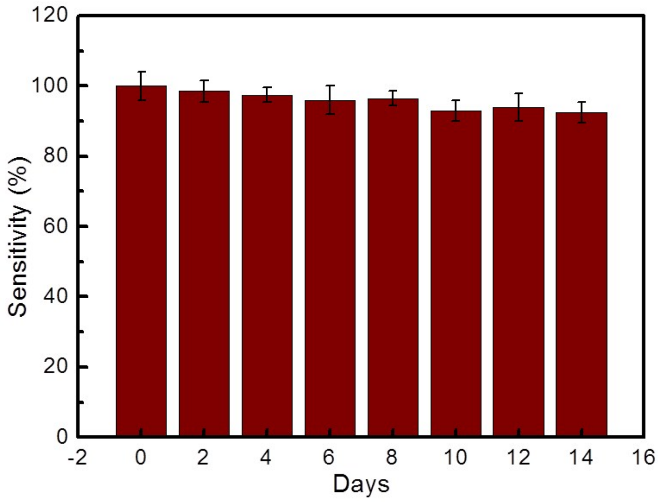

Fig. S6 The long-term stability was evaluated by measuring the CV response to 5 mM DA every two days for two weeks. The electrode was cleaned by DI water and then stored at 4 ℃ after used. Meanwhile, the DA solution for test was refilled at each measurement. Finally, almost 90% of its initial value was remained.

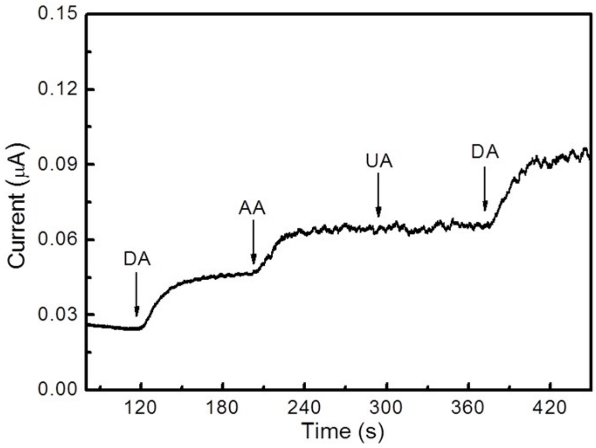

Fig. S7 Amperometric i-t response to the addition of 10 μM DA, AA and UA on the GCE modified with Co_3O_4. Significant increase of the current is observed not only when DA is added but also when AA is added. Additionally, the increase caused by the addition of UA can never be ignored.

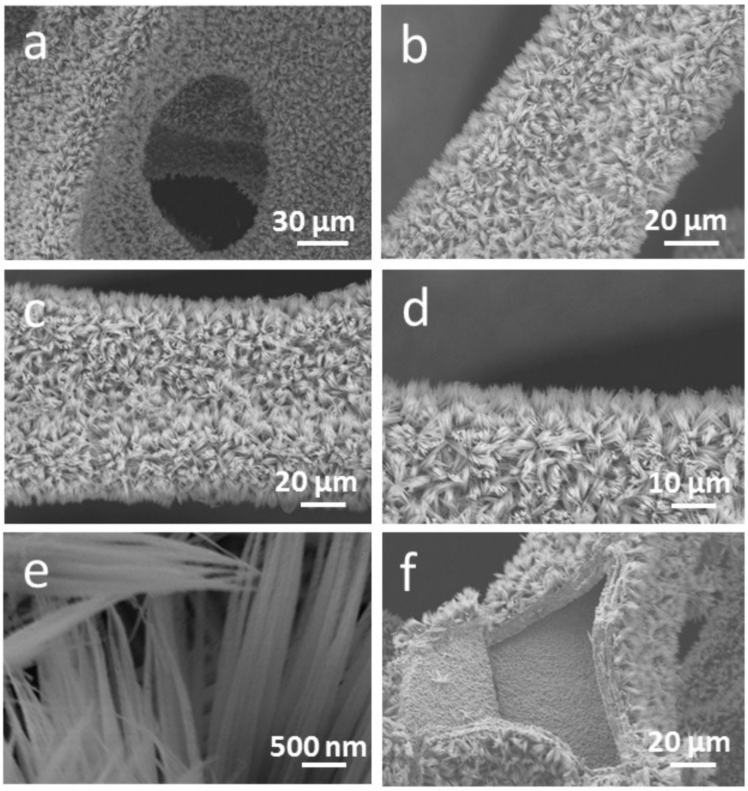

Fig. S8 Low to high magnification SEM images of the NiO foam covered by a layer of dense Co_3O_4 nanoflowers (dense NiO/Co_3O_4 foam).

The 3D interconnected network with amounts of pores can also be observed clearly (Fig. S8a). The NiO almost cannot be observed as coated by a layer of dense Co_3O_4 nanoflowers (Fig. S8b-d). The dense needle-like nanowires are widely distributed, forming a crisscrossed network (Fig. S8e). Especially, the overall structure remains intact even if the skeleton is destroyed by external force (Fig. S8f), indicating the excellent mechanical stability of the prepared self-supporting 3D architecture.

$$Co^{2+} + xF^{-} \rightarrow [CoF_x]^{(x-2)-} \quad (1)$$

$$H_2NCONH_2 + H_2O \rightarrow 2NH_3 + CO_2 \quad (2)$$

$$CO2 + H_2O \rightarrow CO_3^{2-} + 2H^{+} \quad (3)$$

$$NH_3{\bullet}3H_2O \rightarrow NH_4^{+} + OH^{-} \quad (4)$$

$$[CoF_x]^{(x-2)-} + 0.5(2-y)CO_3^{2-} + yOH^{-} + nH_2O \rightarrow Co(OH)_y(CO_3)_{0.5(2-y)}{\bullet}nH_2O + xF^{-} \quad (5)$$

$$Co(OH)_y(CO_3)_{0.5(2-y)}{\bullet}nH_2O + O_2 \xrightarrow{\text{Anneling}} Co_3O_4 + (3n + 1.5y)H_2O + 1.5(2-y)CO_2 \quad (6)$$

Fig. S9 The involved chemical reactions in the preparation of the Co_3O_4 nanoflowers.